Volume 299, number 3, 255–261 FERS 10822 March 1992

Solution conformation of a cyclic pentapeptide endothelin antagonist

Comparison of structures obtained from constrained dynamics and conformational search

Stanley R. Krystek Jr.[a], Donna A. Bassolino[a], Robert E. Bruccoleri[a], John T. Hunt[b], Michael A. Porubcan[c], Charles F. Wandler[d], Niels H. Andersen[d]

[a]*Department of Macromolecular Modeling,* [b]*Department of Chemistry, Cardiovascular Agents and* [c]*Department of Core Resources, Bristol-Myers Squibb Pharmaceutical Research Institute, Princeton NJ 08543-4000, USA* and [d]*Department of Chemistry, University of Washington, Seattle, WA 98195, USA*

Received 23 December 1991; revised version received 31 January 1992

The structure of a cyclic pentapeptide, cyclo-(D-Trp-D-Asp-L-Pro-D-Val-L-Leu), that has high selectivity for the endothelin ET_A receptor has been determined by NMR spectroscopy using constrained molecular dynamics and conformational search procedures. Structures obtained using two methods of refinement, namely (i) constrained molecular dynamics; and (ii) systematic searches of conformational space for optimal satisfaction of distance constraints, were compared to those obtained from systematic searches of conformational space without NMR data. The two different procedures of refinement produce similar conformations that are consistent with the NMR distance constraints. Conformational searches for optimal energy without any NMR distance constraints produced several low-energy structures, two of which have essentially the same backbone as those structures derived from distance-constrained procedures and one of these even reproduces several side-chain positions well. The pentapeptide backbone consists of a linked γ- and β-turn conformation, with the leucine and tryptophan as corner residues of the type II β-turn. The side chains are highly ordered both in aqueous solvent and in dimethyl sulfoxide. In aqueous media the leucine side chain is directed towards the indole ring, presumably to reduce the non-polar surface exposure, producing unusual upfield shifts for the methyls (and particularly Hγ). This structural feature was reproduced in one of the structures obtained from conformational searches performed without NMR data. Exhaustive conformational searches appear to provide an alternative method for structure generation for cyclic peptides.

Endothelin; NMR; Molecular dynamics; Conformational search; Three-dimensional structure; Cyclic pentapeptide

1. INTRODUCTION

We report on recent NMR experiments and computational studies aimed at deriving the three-dimensional structure of a cyclic pentapeptide, a competitive endothelin (ET) antagonist [1–2]. Endothelin, a 21 amino acid peptide originally isolated from porcine endothelial cells [3], has been found to possess a variety of autocrine, paracrine and endocrine functions which modulate the cardiovascular system [4]. The cloning and expression of endothelin genes have identified three isoforms, (ET-1, ET-2, ET-3) [4] with distinct specificities for receptor subtypes (ET_A and ET_B) [5,6]. Recently, a novel cyclic pentapeptide, cyclo(-D-Trp-D-Glu-L-Ala-D-Ile-L-Leu), was isolated from the fermentation products of *Streptomyces misakiensis* and was shown to be a competitive ET_A-selective endothelin antagonist [1]. Peptide syntheses and testing based on this natural lead produced an improved antagonist, cyclo (-D-Trp-D-Asp-L-Pro-D-Val-L-Leu) [2]. Previously, we determined the solution conformation of endothelin [7] in an attempt to explore the conformational dynamics [8] and structure–function relationships of this peptide.

In this manuscript we report the 3D structure for cyclo(-D-Trp-D-Asp-L-Pro-D-Val-L-Leu). Techniques available for structure derivation from NMR-derived interproton distances include metric matrix distance geometry [9–11], variable target functions in torsion angle space [12], restrained molecular dynamics [13,14], simulated annealing [15], and Monte Carlo calculations [16]. In the present work we employed both distance-constrained molecular dynamics, and a newly developed procedure, namely, an exhaustive search of conformational space evaluated for optimal satisfaction of distance constraints [17]. Structures obtained from exhaustive conformational searches without NMR data are compared to the NMR structure.

Correspondence address: S.R. Krystek Jr., Department of Macromolecular Modeling, Bristol-Myers Squibb Research Institute, P.O. Box 4000, Princeton, NJ 08543-4000, USA. Fax: (1) (609) 252-6030.

2. EXPERIMENTAL

2.1. *Experimental methods*

Cyclo-(D-Trp-D-Asp-L-Pro-D-Val-L-Leu) was prepared by conventional solution phase synthesis beginning with *N*-(*t*-butoxycarbonyl)-L-proline phenacyl ester (Boc-Pro-Pac), prepared from a reaction of

Boc-Pro-OH with 2-bromoacetophenone and K_2CO_3 in *N,N*-dimethylformamide (DMF). Standard successive deprotections with trifluoroacetic acid (TFA) and couplings using ethyl-3-(3-dimethylamino)propyl carbodiimide hydrochloride and hydroxybenzotriazole afforded Boc-D-Val-Leu-D-Trp(CHO)-D-Asp(Bn)-Pro-Pac. Following C-terminal deprotection (Zn, AcOH, 40°C), and N-terminal deprotection (TFA), the peptide was cyclized using diphenylphosphoryl azide in DMF with *N*-methylmorpholine. Side chain deprotection was accomplished by hydrogenolysis (Pd/C) followed by base treatment (0.4 M NaOH, 2 min). Preparative gradient HPLC (CH_3CN/H_2O, 0.1% TFA) afforded cyclo(-D-Trp-D-Asp-L-Pro-D-Val-L-Leu) as a white lyophilizate, which was characterized by ^1H- and ^{13}C-NMR, IR, MS and elemental analysis.

The cyclic peptide was examined by NMR in 3 media over a range of temperatures: (i) 12 mM in d_6-dimethylsulfoxide (DMSO), 290–310 K; (ii) 12 mM in 60% aqueous ethylene glycol ('glycol'), 295–310 K; and (iii) 15 mM in 60% aqueous trifluoroethanol (TFE), 295–310 K. For well resolved proton resonances coupling constants were obtained by first order splitting analysis. For the aqueous glycol media (with both H_2O and D_2O), coupling constants were extracted from 4K E-COSY spectra [18,19], which also confirmed the assignment. In aqueous ethylene glycol media, NOE intensities were extracted as previously described [8] from a 2K complex × 240 t_1s phase sensitive (hypercomplex) NOESY spectrum which was zero-filled to a 1K × 1K matrix. In the case of d_6-DMSO, the only media in which the backbone-NH peaks and Pro-αH (unobscured by a shift coincident water peak) occurred, NOE intensities were derived from one-dimensional ΔNOE experiments (τ_m = 200–500 ms) [20], and scaled to the NOESY data based on the integrated size of the residual inverted peak. The final structure elucidation employed only four constraints involving HN/Pro-αH pairs; all other constraints derive from a single NOESY experiment in aqueous glycol.

2.2. *Computational methods*

NOE intensities were converted to initial constraints (d_{ij}) assuming isotropic motion and no spin diffusion; thus d_{ij} is equated with $[r_{ref}(S_{ref}/S_{ij})^{1/6}]$. The shortest $d_{\alpha N}$ connectivity, Leu-α/Trp-HN, was used as the reference set at 2.1 Å, the closest allowed approach distance. Bounds limits – typically ±0.15 at d_{ij} < 3 Å, ±0.30 at d_{ij} 3.0–3.6 Å, and ±0.45 at the extreme reach of the NOE – were established so as to keep all NOE distances within the ranges allowed by holonomic constraints [21]. For a molecular of this size, secondary NOEs are significant only for geminal pairs, such distances were refined using the DISCON algorithm [8,21].

Three-dimensional structures were generated from the NMR data using two different methods. In the first method, distance-constrained molecular dynamics calculations using a simulated annealing protocol [15] as implemented in DISCOVER (version 2.7, Biosym Technologies Inc.), running on Silicon Graphics 4D/440 Workstation was used for structure generation. A variety of starting structures were subjected to 72.5 ps of simulated annealing at 900 K (maximum NOE force constant, 80 kcal·mol^{-1}·Å^{-2}; with a 50 kcal/constraint limit), cooled to 300 K, and minimized using a steepest descent algorithm (7 kcal·mol^{-1}·Å^{-2} for NOEs).

The second method was an exhaustive conformational search as implemented in the program, CONGEN [22]. The method consists of a nested set of iterations over the following steps: (i) a search of the backbone torsion angles ϕ and ψ for each possible dipeptide unit sampling with either a 15° or 10° grid and ω sampled over *cis* and *trans* isomers. Sets of ϕ, ψ, and ω were limited to those having a Van der Waals energy within 5 kcal/mol of the minimum possible; (ii) the modified Go and Scheraga [23] chain closure algorithm applied over the remaining three residues; (iii) 50 steps of Adopted Basic Newton-Raphson energy minimization applied over all resulting conformers; (iv) construction of side chains using the iterative method of Brucoleri and Karplus [22] and a 30° grid on the χ^i angles. These searches correspond to the five possible modes of loop closure for a cyclic pentapeptide. Independent searches were performed both with and without NMR-derived constraints at both 10° and 15° backbone torsion resolution. NMR constraints were incorporated into the search by adding a skewed biharmonic NOE penalty function [7] to the energies in steps 3 and 4.

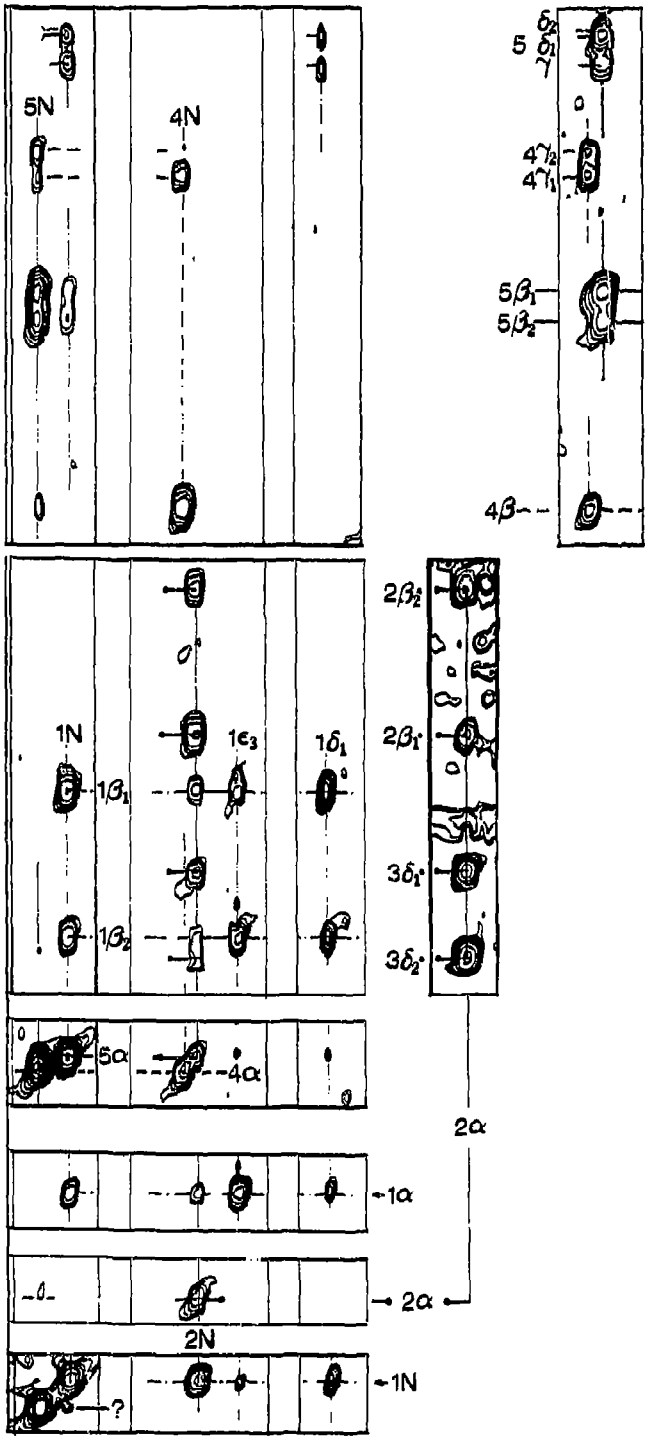

Fig. 1. Strips from the NOESY spectrum of cyclo-(D-Trp-D-Asp-L-Pro-D-Val-L-Leu) in 60% aqueous ethylene glycol. The illustrated strips include all of the backbone NHs, the Asp-Hα and the upfield portion of the Val-Hα and Leu-Hα connectivities.

3. RESULTS AND DISCUSSION

The NMR spectra of the cyclic pentapeptide were readily and unambigously assigned using the standard COSY/NOESY comparison technique [24]. Population analysis based on α/β coupling constants indicated that a single χ^1 rotomer predominated in each side chain, for the Leu side chain particularly in aqueous media. The sharp doublet Pro-Hα resonance revealed the pucker of the proline ring and allowed a full stereospecific assignment from *cis/trans* relationships evident in the E-COSY and NOESY spectra. The stereospecific assignment for valine is for the χ^1 conformer with αH and βH antiperiplanar. A preliminary conformational search revealed that the solvent sequestration of 4-HN and 2-HN (signalled by temperature gradient more positive than −4 ppb/°C), the established proline pucker, and the two very large $d_{\alpha N}$ connectivities (4α/5HN and 5α/1HN) could be accommodated only for a subset of ϕ/ψ values over which an unambiguous prochirality assignment could be made from NOE ratios using the intra-residue and sequential HN connectivities of the Leu, Trp, and Asp side chain protons. The complete assignment appears in Table I. Portions of the NOESY spectrum appear as Fig. 1.

Sixty-three conformationally significant non-zero NOEs were converted to distance bounds. An additional 17 unobserved NOEs were converted to low-bounds-only constraints. Of the full set of 80 bounds: 42 reflected predominantly the backbone, and 38 involved more remote side-chain interactions. The final structures from distance-directed dynamics and search protocols displayed no violations of backbone constraints exceeding 0.4 Å (typically the average absolute violations were < 0.05 Å). Six constraints involving the remote regions of the Trp and/or Leu side chains could not be fitted (violations > 0.5 Å) with any single conformer – $1\delta_1/5\delta^*$ (3.2–4.4), $1\alpha/1\varepsilon_3$ (3.2–4.2), $1\delta_1/1\beta_2$ (2.4–3.3), $1\delta_1$/1HN (2.5–3.3), $1\varepsilon_3/1\beta_2$ (3.0–3.9), $5\alpha/5\delta_2$ (3.0–3.9 Å). This failure likely reflects residual side-chain motion (Trp-χ^2 and Leu-$\chi^{1,2}$) and we exclude these constraints from the statistical comparisons and they were also excluded from the steepest descent minimization of the structures.

Ten structures each were generated by simulated annealing and conformational search based on the NOE constraints. Table II shows the variations in backbone dihedrals, range of predicted αH/HN coupling constants, and key NOE distances observed for these structures. Figure 2 shows the degree of convergence that

Table I

Chemical shifts and coupling constants: cyclo-(D-Trp-D-Asp-L-Pro-D-Val-L-Leu)[a]

	NMR experimental conditions		
	60% glycol, 310K	60% TFE, 295K	d_6-DMSO, 295K
D-Trp			
HN: δ (J_α,$\Delta\delta/\Delta$T)	8.36 (7.6, −10.2)	7.78 (7.5, −5.6)	8.765 (8.0, −5.3)
α; β_1,β_2	4.65; 3.445, 3.065	4.74; 3.495, 3.205	4.275; ~3.32, 2.90
($J_{\alpha\beta1}$),($J_{\alpha\beta2}$)	(3.8), (11.3)	(4.5), (9.7)	(~3), (11.5)
$\varepsilon1$,$\varepsilon3$,$\zeta2$	10.18, 7.60, 7.41	9.64, 7.67, 7.47	10.81, 7.52, 7.32
$\delta1$,$\eta2$,$\zeta3$	7.21, 7.140, 7.065	7.21, 7.225, 7.145	7.17, 7.06, 6.96
D-Asp			
HN: δ (J_α,$\Delta\delta/\Delta$T)	7.67 (8.9, −3.4)	7.515 (9.1, −3.45)	7.71 (9.2, −1.9)
α; β_1, β_2	5.07; 2.905, 2.495	5.145; 2.80, 2.475	4.98; 2.795, 2.34
($J_{\alpha\beta1}$),($J_{\alpha\beta2}$)	(9.8), (4.7)	(9.7), (4.8)	(10.3), (4.1)
L-Pro			
α: δ ($J_{\alpha\beta1}$,$J_{\alpha\beta2}$)	4.85 (<1.2, 7.8)[b]	4.825 (<1.2, 7.6)	4.765 (<1.2, 7.9)
δ_1, δ_2	3.28, 3.51	3.415, 3.655	3.15, ~3.34
β_1, β_2; γ_1, γ_2	2.255, 1.77; ~2.00	2.29, 1.85; ~2.075	2.265, 1.61; 1.77, 1.93
D-Val			
HN: δ (J_α,$\Delta\delta/\Delta$T)	7.725 (9.9, −0.98)	7.955 (9.9, −1.76)	7.50 (10.3, −0.34)
α, β ($J_{\alpha\beta}$)	4.005, 1.79 (9.0)[c]	3.96, 1.89 (~9)	4.145, 1.68 (8.0)[c]
γ_1, γ_2	0.91, 0.855	0.955, 0.89	0.865, 0.83[d]
L-Leu			
HN: δ (J_α,$\Delta\delta/\Delta$T)	8.46 (5.0, −7.8)	7.985 (5.0, −7.4)	8.755 (5.8, −4.3)
α; β_1, β_2	3.96; 1.23, 1.31	~3.97; 1.31, 1.395[d]	3.995; 1.15, 1.225[d]
($J_{\alpha\beta1}$),($J_{\alpha\beta2}$)	(6.2), (9.7)	(~6), (~8)	(~6.2), (~8.4)[d]
γ; δ_1, δ_2	0.665; 0.545, 0.52	0.82; 0.62, 0.605[d]	1.02; 0.73, 0.615[d]

[a] Chemical shifts are reported to the nearest 0.005 ppm; coupling constants are accurate to ± 0.4 Hz; HN shift temperature gradients are given in ppb/°C.

[b] For the aqueous glycol media, the Pro-αH data was obtained from a comparable experiment in 60%-d-glycol/D_2O: the Pro-αH was completely coincident with the H_2O signal and thus bleached in the other experiment.

[c] Population analysis, fraction with χ^1_{Val} = +60°[θ(Hα/Hβ)=−180°]: 0.65(aq. glycol), 0.55 (DMSO).

[d] Stereospecific assignment not fully confirmed.

resulted for the two procedures. RMSD comparisons and NOE violations among each group of structures and between protocols are given in Table III. Two structures generated by a conformational search without NOE constraints (vide infra) are also included. These resemble the CONGEN structures rather than those obtained with DISCOVER. Data in the Tables can be summarized as follows. Two similar, but distinctive, structures have been produced. The DISCOVER-generated structures display a slightly better fit to the NOE distances. However, additional NMR data provide another basis for selecting a best-fitting hypothesis. Once it is established (as in this case) that ϕ values are not extensively averaged, observed values of $J_{N\alpha}$ can be used as an additional criterion for model correctness. As can be seen in Table II, the conformational search gave structures which more accurately predict the observed ϕ-dependent coupling data. We selected the CONGEN structure with the lowest NOE violations as the final model for the RMSD comparisons in Table III and structure comparisons in Fig. 3. It appears as Panel A in Fig. 3. Panel B shows DISCOVER-generated structures (with and without the inclusion of ϕ constraints used to improve the correlation between predicted and observed $J_{N\alpha}$ values) overlaid on the final model. Panel C shows two structures from systematic searches performed without NMR data overlayed on the structure in Panel A. Exhaustive conformational searches performed without NMR data were attempts to predict, a priori the conformation of this cyclic peptide.

The conformation adopted by this cyclic pentapeptide can be described as a type II β-turn over D-Val-Leu-D-Trp-D-Asp with an inverse γ-turn completing the ring, a motif previously noted for cyclo(D-D-Pro-L) peptides [25,26]. The valine and aspartate amide-NHs display low temperature gradients in all solvents examined, however the hydrogen bonds are not highly persistent since exchange with D_2O occurs in 5 min or less at pH 3. The unusual variability of the gradient for the Trp-NH likely reflects shift changes due to the changing disposition of the indole ring in equilibrating side-chain conformers [8]. Both the modeling results and the NMR data provide a compelling argument for the population

Table II

Comparison of calculated and experimental constraints[a,b]

Residue	DISCOVER dynamics	CONGEN search	Experiment
D-Trp			
ϕ	+83 (3)	+81 (12)	–
$J_{N\alpha}$	7.1 (0.6)	6.9 (1.5)	7.7 (0.4)
ψ	+15 (6)	+27 (3)	–
1Hα/2HN	3.44 (0.04)	3.50 (0.02)	3.25–3.65
D-Asp			
ϕ	+145 (5)	+150 (9)	–
$J_{N\alpha}$	8.7 (0.8)	8.2 (1.5)	9.0 (0.4)
ψ	−90 (3)	−94 (7)	–
2Hα/3HN	2.25 (0.05)	2.30 (0.08)	2.2–2.6
L-Pro			
ϕ	−81 (8)	−81 (2)	–
ψ	+40 (21)	+51 (9)	–
3Hα/4HN	2.91 (0.28)	2.56 (0.09)	2.45–2.9
D-Val			
ϕ	+127 (7)	+128 (10)	–
$J_{N\alpha}$	10.3 (0.5)	10.1 (0.8)	10.0 (0.4)
ψ	−119 (6)	−126 (18)	–
4Hα/5HN	2.09 (0.05)	2.15 (0.05)	2.05–2.25
L-Leu			
ϕ	−105 (6)	−76 (12)	–
$J_{N\alpha}$	9.6 (0.6)	6.2 (1.6)	5.3 (0.5)
ψ	+124 (7)	+107 (10)	–
5Hα/1HN	2.11 (0.04)	2.10 (0.02)	2.0–2.2
β Turn character			
5α/2HN	3.56 (0.20)	3.75 (0.07)	3.0–3.6
1HN/2HN	2.71 (0.07)	2.49 (0.16)	2.2–2.55

[a] Values in parentheses are standard errors for distances and angles. For coupling constant estimates the error is selected to include the full range of predicted values over the ensemble of structures.

[b] Model values deviating from the experimental are underlined. These also serve to highlight the differences between the DISCOVER and CONGEN models.

Table III

Comparison of structures and constraint violations[a]

Superimposition	DISCOVER dynamics	CONGEN NOE-weighted	CONGEN unweighted
Backbone rmsd (each group)	0.21 (0.09)	0.28 (0.13)	ND[b]
Heavy atom rmsd (each group)	0.85 (0.51)	0.40 (0.14)	ND[b]
Backbone rmsd (final model)	0.43 (0.05)	0.23 (0.13)	0.22, 0.37
Heavy atom rmsd (final model)	1.06 (0.08)	0.35 (0.13)	0.25, 2.12
Backbone NOEs[c]			
<|viol|>	0.027±0.007	0.039±0.007	0.07, 0.11
largest violation	0.30±0.07	0.24±0.04	0.51, 0.75
Side chain NOEs[d]			
<|viol|>	0.067±0.040	0.056±0.007	0.07, 0.22
largest violation	0.48±0.07	0.53±0.15	0.32, 1.23

[a] Ten structures obtained from constrained dynamics using DISCOVER, ten structures obtained from conformational searches using distance constraints, and the two structures obtained from conformational searches without distance constraints are compared. A total of ten structures were generated from the CONGEN searches without NMR data, however only two (at 10° and 15° grid increments) from a single loop closure mode produced a backbone similar to the NOE-derived models. The other loop closure modes produced structures with an average backbone constraint violation between 0.19 and 0.38 Å.

[b] ND = not determined.

[c] Average violation over 36 backbone distance constraints, units are in Å.

[d] Average violation over 37 side chain distance constraints, units are in Å.

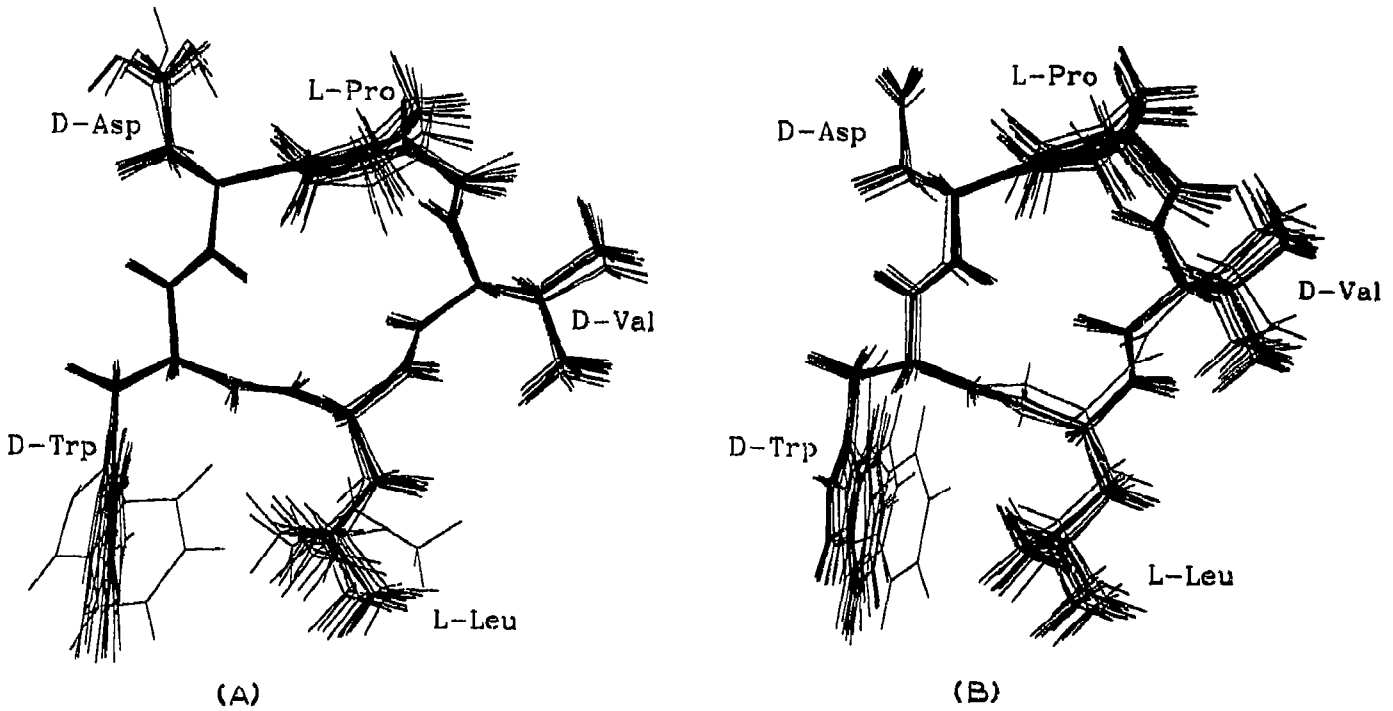

Fig. 2. *Panel A*, ten DISCOVER-generated structures from simulated annealing based on 80 NOE constraints. *Panel B*, ten structures from conformational searches evaluated for optimal satisfaction of distance constraints. Each set is least squares overlaid for the backbone atoms and appear in the same perspective.

of a conformer with a hydrophobic cluster in which the Trp indole ring shields the leucine side chain from aqueous exposure. The Leucine side chain becomes more disordered in d_6-DMSO and in the membrane-mimicking media, 60% TFE. There appears to be some analogy to the endothelin C-terminus. In the case of endothelins (and sarafotoxin 6b), one of the methyl groups in residue 19 appears at unusually low chemical shift and large NOE connectivities between residues 19 and 21 are observed [8,27,28]. The structuring of the C-terminus of endothelins in aqueous media may be governed by a similar hydrophobic interaction. Further studies of this cyclic pentapeptide endothelin antagonist and comparative modeling of the C-terminus of ET-1 are underway and should provide hypotheses for binding requisites and stereochemistry at the ET_A receptor.

REFERENCES

[1] Ihara, M., Fukuroda, T., Saeki, T., Nishikibe, M., Kojiri, K., Suda, H. and Yano, M. (1991) Biochem. Biophys. Res. Commun. 178, 132–137.
[2] European Patent Application (1990) Application Number 90124947.4, Publication Number 0 436 189 A1.
[3] Yanagisawa, M., Kurihara, H., Kimura, S., Tomobe, Y., Kobayashi, M., Mitsui, Y., Yazaki, Y., Goto, K. and Masaki, T. (1988) Nature 332, 411–415.
[4] Rubanyi, G.M. and Parker Botelho, L.H. (1991) FASEB J. 5, 2713–2720.
[5] Sakurai, T., Yanagisawa, M., Takuwa, Y., Miyazaki, H., Kimura, S., Goto, K. and Masaki, T. (1990) Nature 348, 732–735.
[6] Arai, H., Hori, S., Aramori, I., Ohkuba, H. and Nakanishi, S. (1990) Nature 348, 730–732.
[7] Krystek, Jr., S.R., Bassolino, D.A., Novotny, J., Chen, C., Marschner, T.M. and Andersen, N.H. (1991) FEBS Lett. 281, 212–218.
[8] Andersen, N.H., Chen, C., Marschner, T.M., Krystek, Jr., S.R. and Bassolino, D.A. (1992) Biochemistry, in Press.
[9] Havel, T. and Wuthrich, K. (1985) J. Mol. Biol. 182, 281–294.
[10] Hare, D.R. and Reid, B.R. (1986) Biochemistry 25, 5341–5350.
[11] Guntert, P., Braun, W. and Wuthrich, K. (1991) J. Mol. Biol. 217, 517–530.
[12] Braun, W. and Go, N. (1985) J. Mol. Biol. 186, 611–626.
[13] Brunger, A.T., Clore, M., Gronenborn, A. and Karplus, M. (1986) Proc. Natl. Acad. Sci., USA 83, 3801–3805.
[14] van Gunsteren, W.F. and Berendsen, H.J.C. (1977) Molec. Phys. 34, 1311–1327.
[15] Nilges, M., Gronenborn, A.M., Brunger, A.T. and Clore, G.M. (1988) Protein Eng. 2, 27–38.
[16] Bassolino, D.A., Kominos, D., Kitchen, D.B., Hirata, F., Pardi, A. and Levy, R.M. (1988) Int. J. Supercomputer Applications 2, 41–55.
[17] Bassolino, D.A. and Bruccoleri, R.E., in Preparation.
[18] Griesinger, C., Sorensen, O.W. and Ernst, R.R. (1987) J. Magn. Reson. 75, 474–481.
[19] Driscoll, P.C., Clore, G.M., Beress, L. and Gronenborn, A.M. (1989) Biochemistry 28, 2178–2187.
[20] Andersen, N.H., Nguyen, K.T., Hartzell, C.J. and Eaton, H.L. (1987) J. Magn. Reson. 74, 195–203.
[21] Andersen, N.H., Lai, X. and Marschner, T. (1991) NOESYSIM/DISCON Documentation, copyrighted by the University of Washington.
[22] Bruccoleri, R.E. and Karplus, M. (1987) Bioploymers 26, 137–168.

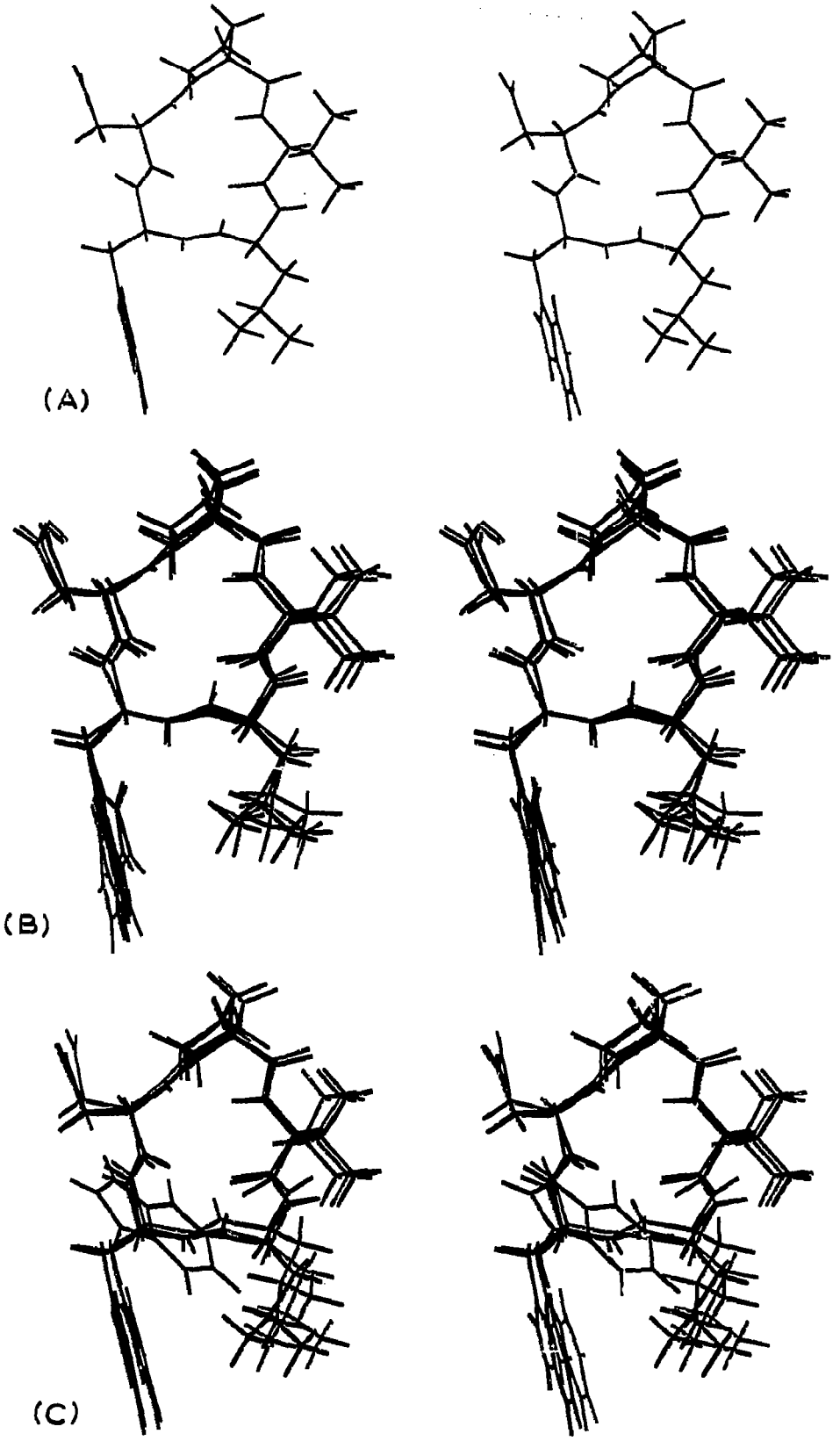
(A)
(B)
(C)

[23] Go, N. and Scheraga, H.A. (1970) Macromolecules 3, 178–187.
[24] Wuthrich, K. (1986) NMR of Proteins and Nucleic Acids, John Wiley and Sons, New York.
[25] Stradley, S.J., Rizo, J., Bruch, M.D., Stroup, A.N. and Gierasch, L.M. (1990) Biopolymers 29, 263–287.
[26] Kessler, H., Kutscher, B. and Klein, A. (1986) Liebigs Ann. Chem. 893–913.
[27] Bortmann, P., Hoflack, J., Pelton, J.T. and Saudek, V. (1991) Neurochem. Int. 18, 491–496.
[28] Mills, R.G., Atkins, A.R., Harvey, T., Junis, F.K., Smith, R. and King, G.F. (1991) FEBS Lett. 282, 247–252.

←
Fig. 3. *Panel A*, the stereo pair of the best fitting CONGEN model. *Panel B* shows a stereo view of two DISCOVER-generated structures overlaid on the structure in Panel A. The structure colored cyan was obtained without ϕ constraints. The magenta colored structure was generated including ϕ torsion drivers (20 kcal/radian^2) which favor the values required by the NH/αH coupling constants. The resulting structures (one of which is illustrated) showed comparable low violation of both the backbone NOE constraints [<viol> = 0.03 Å, maximum single violation = 0.29 Å] and side chain constraints. The basis for the failure of DISCOVER-generated models to reach this conformation in the absence of ϕ constraints remains unclear. The center averaging (rather than r^{-6}-averaging) of methyl constraints in DISCOVER appears to contribute to the problem. The differences between DISCOVER-generated structures and CONGEN structures are highlighted in Table II. *Panel C*, stereo view of two structures (red and green) from CONGEN searches without NMR data are overlaid on the best-fit structure from the searches with NMR data (the model in Panel A).